Boundary Element Energy Method: an efficient tool for acoustic computation

Michael Thivant, Aurélien Cloix, Christian Clerc, N. Blairon, C. Braguy

10ème Congrès Français d'Acoustique
Lyon, 12-16 Avril 2010

Boundary Element Energy Method : an efficient tool for acoustic computation

M. Thivant [1], A. Cloix [1], C. Clerc [1], N. Blairon [2], C. Braguy [2]

[1] VIBRATEC 28, Chemin du Petit Bois, 69131 ECULLY Cedex, France michael.thivant@vibratec.fr
[2] VOLVO 3P, API TER H50 1 22, 1 avenue Henri Germain, 69802 SAINT PRIEST Cedex, FRANCE

The acoustic prediction for transportation vehicles (ground transportation, aeronautics, naval application) at design stage is an increasing issue for the industry. Due to reduced development times, the acoustic design must start in the early stage of projects and follow the whole development phase, requiring precise and reactive prediction tools. The most widely used computation methods perform a numerical resolution of Helmholtz equation with a spatial discretization into Finite Elements or Boundary Elements. These methods are efficient in the low frequency range, but they reach their limits at higher frequencies, due to high computational cost, very precise mesh required, and high sensitivity to geometry and frequency. Ray Tracing techniques may be an alternative in some cases, but diffuse reflection is generally ignored and convergence is not always reached. The method proposed here is also based on a light/sound analogy, but the resolution is based on acoustic intensity equilibrium on Boundary Elements. Acoustic domain boundaries (Walls and structures) are modelled by finite elements for which physical properties are the absorption and transmission coefficients. The mesh size is led only by the geometry description and is not frequency dependent: thus the computation time is drastically reduced. Transparency phenomenon and internal noise issue have been recently implemented in the method in order to compute multi-domain acoustic fluid. This energy method is dedicated to acoustic issues in the mid and high frequency range, preferably with complex geometries, broadband and distributed sources. The acoustic resolution is carried out by recently developed software SONOR. After the method description, some applications on thermal engines shields and on cabin interior noise are presented and the results are discussed.

1 Introduction

The prediction of acoustic shields efficiency is of great interest in machinery and vehicle noise control. Classical methods based on Helmholtz's equation are quite accurate in low frequencies and for simple geometry, but they are limited for industrial problems by their computing time and their lack of robustness. To overcome these difficulties, a method inspired by both Ray-Tracing techniques and Energy-based Boundary Elements methods is proposed here.

2 Basic theory

From Sabine diffuse field model [11] to acoustic ray tracing techniques, the analogy with light propagation phenomena has been widely used to model high frequency sound propagation.

The model proposed here uses surface boundary elements to describe sources, absorbing and reflecting surfaces. Based on energetic quantities and energy balance, the spirit of SEA is conserved, but unlike SEA the repartition of energy density can be predicted. Theoretical details can be found in references [6] to [10].

2.1.1 Equivalences

The analogy is based on the equivalence between sound and light intensities:

$$\vec{I}_{light}=\vec{I}_{sound}=\vec{I} \quad (1)$$

Acoustic sources are represented by light sources, with an equivalent power (in Watt) imposed on the area of the elements representing the source.

The incident intensity on boundary elements is partly reflected, and partly absorbed. Here again, the analogy between light and acoustic diffuse absorption coefficients is straightforward:

$$\alpha_{light}=\alpha_{sound} \quad (2)$$

The energy exchanged by a couple of boundary elements depends on their mutual "view factor". This factor is only related to geometry (elements area, orientation, presence of obstacle between the 2 boundary elements). The concept of view factors can then be applied to both light and sound propagation: the view factor dF_{QP} between "source" dS_P and "receiver" dS_Q is the fraction of power emitted by dS_P and viewed by dS_Q. In the absence of obstacle between dS_P and dS_Q, dF_{QP} can be written:

$$dF_{QP}=\frac{\cos\theta_P\cos\theta_Q}{\pi\left|\vec{R}_{PQ}\right|^2}dS_P \quad (3)$$

For a closed surface S_P the global view factor respects the power balance:

$$\oiint F_{QP}=1 \quad (4)$$

Surfaces dS_P and dS_Q can be at the same time "source" and "receiver" for each other. The reciprocal view factors dF_{QP} and dF_{PQ} are related by:

$$dF_{QP}dS_Q=dF_{PQ}dS_P \quad (5)$$

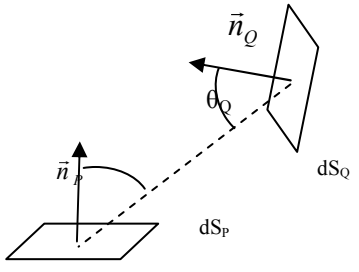

Figure 1 View factors

2.1.2 Model assumptions

The assumptions used are the following:

Uncorrelated waves are assumed: interferences between waves are neglected. This assumption is valid for acoustic problems at high frequencies, with broadband sources and complex environments.

Sources are described by their emitted power (direct analogy between acoustic and light power). Sound power is uniformly distributed on source surface and radiate diffusely in all directions.

The incident field on each element is diffuse.

Diffuse absorption: if an element i receives a power $w_{incident}(i)$ from the other elements (either direct radiation from sources or reflected by other boundary elements) it will absorb part of the incident power:

$$w_{absorbed}(i)=\alpha_i\, w_{incident}(i) \quad (6)$$

Where α_i is the absorption coefficient of the surface in diffuse field.

Diffuse reflection: the element i will radiate uniformly the reflected power defined by equation 7, according to their view factors to the other surfaces (as illustrated in Figure 2). r_i is the reflection coefficient on element i.

$$w_{reflected}(i) = r_i\, w_{incident}(i) \quad (7)$$

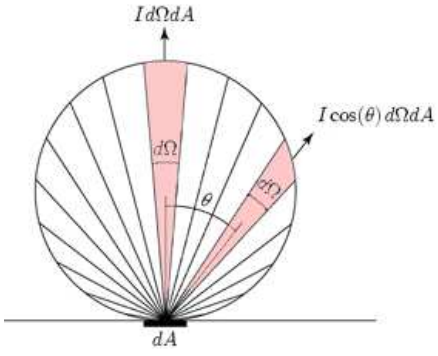

Figure 2 Diffuse reflection (Lambert's Law)

Diffuse transmission : the power transmitted from face k to face i of an element is given by equation (8), where τ_{ki} is the transmission coefficient in diffuse field.

$$W_{Transmitted}(i) = \tau_{ki} * W_{incident}(k) \quad (8)$$

The coefficients of absorption, reflection and transmission are related together by equation 9, deriving from power balance on element i.

$$1 = \alpha_i + \tau_{ik} + r_i \quad (9)$$

Diffraction: to date, the methodology does not include diffraction effects on the edges of boundary elements. Nevertheless, the diffraction effects could also be introduced, but needs more research efforts [10].

As a result, the pressure level in shadow zone could be underestimated by the method.

2.1.3 Power balance

To derive the system of equations to be solved, the power balance is written on each boundary element.

For acoustic problems the power w(i) emitted by the element i is the sum of reflected, transmitted and source powers:

$$w(i) = W_{Reflected}(i) + W_{Transmitted}(i) + W_{Source}(i) \quad (10)$$

The reflected and transmitted powers are expressed in terms of incident powers using equations 7, 8.

On the other end, the incident power $w_{incident}(i)$ is the sum of the powers w(j) emitted by the other elements j, weighted by the view factors F_{ji}:

$$w_{incident}(i)=\sum_{j\neq i} F_{ji}\, w(j) \quad (11)$$

Introducing equations 7, 8 and 11 in equation 10 gives:

$$w(i) = (1-\alpha_i-\tau_{ik})\sum_{j\neq i} F_{ji}\, w(j) + \tau_{ki}\sum_{j\neq k} F_{jk}\, w(j) + W_{Source}(i) \quad (12)$$

One obtains a system of n equations (with n the number of boundary elements), with n unknowns being the powers emitted by each elements.

2.2 View factors computation

The first step is to compute the view factors F_{ij}. A shadowing check must be processed to identify pairs of elements having obstructed views. The exact solution given by equation 13 is used to compute view factors between pairs of element with unobstructed views.

$$Ai\,.\,Fij = Aj\,.\,Fji = \frac{1}{\pi}\iint_{AjAi} \cos\theta_i \cos\theta_j \frac{dAidAj}{r_2} \quad (13)$$

For element pairs partially shadowed by other elements, the hemicube method is used. This technique is embedded in NASTRAN MARC software.

2.3 Acoustic resolution using SONOR software

VIBRATEC has developed a C^{++} software called SONOR to handle pre-processing, acoustic computation and post-processing.

For each frequency step f, a matrix M(f) is built according to equation (14), where I is the identity matrix, $\alpha_i(f)$ is the diffuse absorption coefficient, τ_{ik} and τ_{ki} are respectively the transmission coefficient from face i to face k, and from face k to face i of a given element.

$$M_{ij}(f) = I - (\alpha_i + \tau_{ik})F_{ji} + \tau_{ki}F_{jk} \quad (14)$$

The vector $w_i(f)$ of the emitted power for element i at frequency step f) is obtained by multiplying the inverse matrix $M^{-1}(f)$ by the source vector w_{Si}. In case of multiple load case (successive sources defined by groups of elements), the source vector w_{Si} becomes a source matrix noted W_{Sis} and the solution is a matrix W_{is} of emitted powers, where the row index i is related to the element number and the column index s corresponds to the load case.

$$W_{is}(f) = M_{ij}^{-1}(f) * Ws_{is} \quad (15)$$

Thus the inversion process, which is the most time consuming, is done just one time per frequency step, and multiple load cases are handled by matrix notation.

The frequency dependence of the matrix $M_{ij}(f)$ (depending on the reflection coefficient $r_i(f)=1-\alpha_i(f)-\tau_{ik}$), and possibly the frequency dependence of the source powers $w_{si}(f)$, are handled by a loop in the program.

3 Post-processing of the results

3.1 Power levels

The incident power at each boundary element can be derived from the emitted power using equation 11.

The absorbed, reflected and transmitted powers can be derived from the incident power using equations 6 7 and 8.

Any power balance can then be computed on groups of boundary elements, summing either absorbed, reflected,

transmitted or incident powers. This gives local information that can be useful for design optimization: the power absorbed by a given shield, the power transmitted through an aperture, the incident power at a possible location for absorbing material etc.

3.2 Insertion Loss

The Insertion Loss can be computed at a receivers location from the results obtained in two configurations (with absorbing shields / with transparent shields)

$$IL_{computed}(f, source) = 10.*\log\left(\frac{w_{receiver}^{transparent\_shields}}{w_{receiver}^{absorbing\_shields}}\right) \quad (16)$$

3.3 Pressure levels

The acoustic pressure can be estimated from the local intensity using acoustic field assumptions:

• In the case of far-free-field or plane waves:

$$P^2 = I\ \rho_0 c \quad (17)$$

• In the case of diffuse field (Sabine theory):

$$P^2 = I\ 4\rho_0 c \quad (18)$$

• In the case of intermediate sound field, the pressure level at a point receiver is computed by scalar summation of the contribution of all visible element faces:

$$P^2 = \sum_{i=1}^{N} \frac{\cos(\theta_i)}{r_i^2} * W_{emitted}(i) \quad (19)$$

4 Boundary elements model

The boundary elements should describe the geometry accurately enough, but no frequency criteria related to the wavelength is required, unlike standard finite element methods solving Helmholtz equation. Standard element quality checks are however performed and the distance between facing elements should not be lower than the element size.

4.1 Sources mesh

LMS Pre-acoustics software was used to mesh the engine (811 elements) and the engine mesh was distributed into six groups (engine faces) in order to simulate successively six engine sources (see Figure 3).

The boundary condition for the sources is written in terms of emitted power on each element face, proportional to its surface, and resulting in a prescribed power spectrum for the whole group defining the source:

$$\mathrm{w(i)} = W_S \frac{Surface(i)}{\sum_{Source\_group} Surface(j)} \quad (20)$$

Sources elements are also defined by their absorption and transmission coefficients, which are set here to zero.

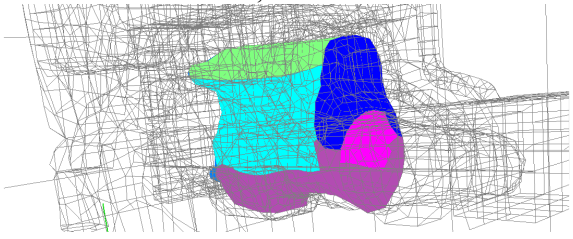

Figure 3 Engine faces groups within the mesh of the truck

4.2 Powertrain environment

The vehicle components might influence the noise propagation from the power train. These components have been included in the Boundary Element Model (see Figure 4 to Figure 5).

Shields elements are distributed in 6 groups according to the local thickness of the shield (see Figure 4):

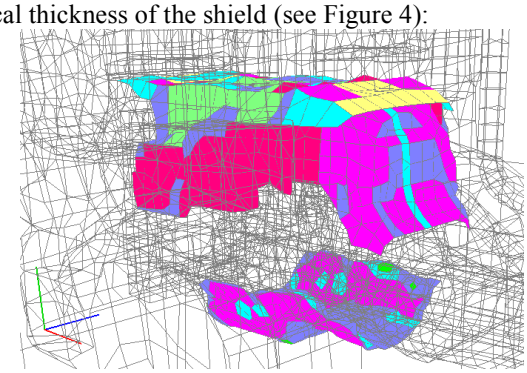

Figure 4 Boundary elements mesh of the shielding – Colours according to cotton felt thickness

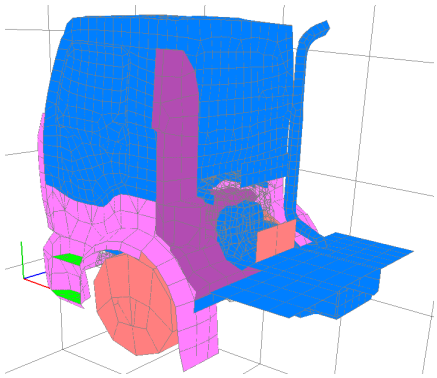

Figure 5 Boundary elements mesh of the truck – Rear view

4.3 Far field mesh

The far field is represented by a cube of 15 m edge length (Figure 6).

For exterior noise issues, the ground is not meshed: its absorption is assumed to be null and therefore the entire incident power on the ground is assumed to be reflected to the far field. In the model this reflected power hits the lower half of the far field cube. For interior noise issues (§6) the ground is meshed with reflecting elements.

Receivers at 7.5m are selected, corresponding to vehicle positions at 12m, 14m and 16m, at which the maximal noise generally occurs. The power radiated to the receivers group, gathering element faces located both above and below the ground, is used to compute the Insertion Loss of the shields.

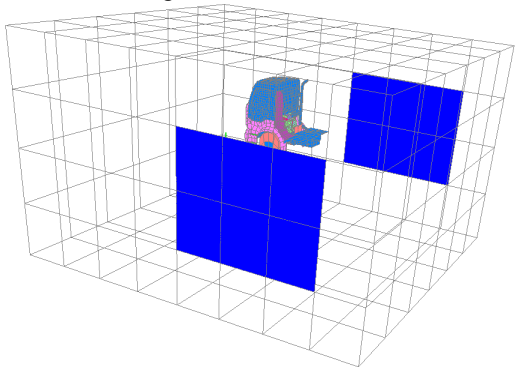

Figure 6 Receivers mesh for Insertion loss computation

4.4 Boundary conditions

4.4.1 Source power

Sources elements groups are used to define sources. Measured power spectra per engine face (see Figure 7) are distributed on each engine face (back, bottom, front, left, right and top). The source matrix W_{si} contains the source power applied to the element i. The source power on each element is computed from eq. 21, in order to have uniform power flux:

$$Ws_i = Ws \frac{surface(elt\_i)}{\sum_{j \in source\_group\_s} surface(elt\_j)} \quad (21)$$

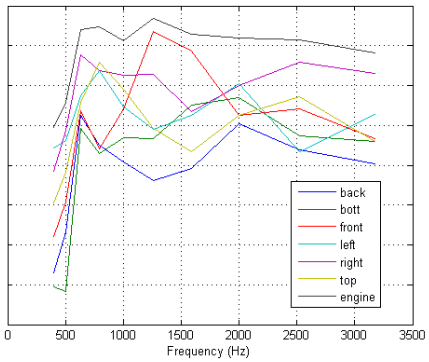

Figure 7 Acoustic power of diesel truck engine faces. (in dBA, 40 dB range). Most of the power is between 500 Hz and 3 kHz, within the method validity range.

4.4.2 Absorption coefficients

The normal impedance Z=R+jX corresponding to cotton felt (2.4 kg/m²) are deduced from BIOT parameters measured by the LAUM during prior PREDIT project.

Then the absorption coefficient at incidence angle θ derives from equation (22).

$$\alpha(\theta) = \frac{4R\cos\theta}{(R\cos\theta + 1)^2 + X^2\cos^2\theta} \quad (22)$$

The diffuse absorption coefficients can be deduced from the average versus the incidence angle θ over 2π solid angle. Note: generally the integration versus θ is limited to [0;78°] rather than [0;90°] to avoid the problem of grazing waves.

$$\langle\alpha\rangle_\theta = \int_0^{\pi/2} 2\alpha(\theta)\cos\theta\sin\theta d\theta \quad (23)$$

Diffuse absorption coefficients are drawn on Figure 8 for thicknesses 5 mm to 30 mm.

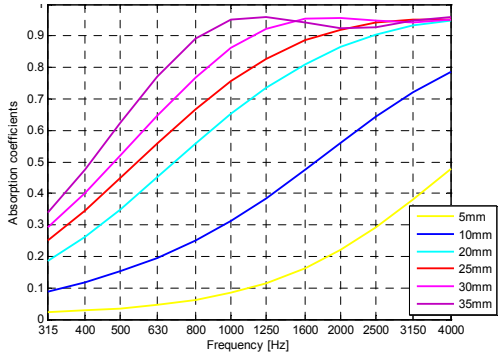

Figure 8 Diffuse absorption coefficient of 2.4 kg/m² cotton felt, computed from the impedance measured by the LAUM (Laboratoire d'Acoustique de l'Université du Maine)

5 Exterior noise results

5.1 Power balance

The method is based on power balances among elements. One important validation of the resolution program consists in checking the general power balance given by equation (24).

$$W_{Source} = \sum_{groups} W_{absorbed} \quad (24)$$

The global power balance is exactly respected for each load case. Moreover, summing the power absorbed by groups of elements (shields, cube faces, eventually receivers) gives physical information on acoustic energy path.

5.2 Insertion Losses

5.2.1 Computed Insertion Losses

The Insertion Loss is computed from equation 16, for each load case, from the ratio between the powers absorbed by the exterior cube with/without the shields.

5.2.2 Measured Insertion Losses

For diesel engine encapsulation (trucks or railway rolling stock applications) the frequency range of interest is approximately from 300 Hz up to at least 3 kHz (Figure 7). Measured Insertion Losses are deduced from transfer function measured on the real truck (Figure 10). The methodology is described in references [4] and [5]. Third-octave quadratic transfer functions P^2/Q'^2 are averaged over each engine faces or the whole engine, and over 6 loudspeakers positions at 7.5m (see Figure 9). Two configurations are considered: with all the shields and without any shield. The measured IL is then derived from equation 25.

$$IL_{measured}(f, source) = 10 * \log 10\left(\frac{(P^2/Q'^2)_{without\_shields}}{(P^2/Q'^2)_{with\_shields}}\right) \quad (25)$$

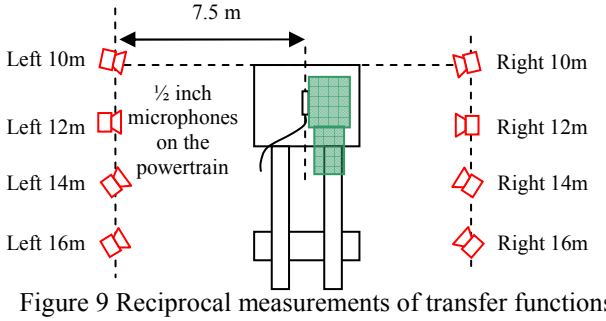

Figure 9 Reciprocal measurements of transfer functions

Figure 10 Transfer function measurement on truck

5.2.3 Insertion Loss comparison

Figure 11 shows both computed and measured Insertion Losses for each engine face, on a Renault Truck vehicle, with a complete set of shields. The trends are correct (order of magnitude, hierarchy of the different engine faces, frequency dependence). Discrepancies below 800 Hz could be explained by modal behaviour.

5.3 Pressure Levels comparison

Pressure levels on certification microphones are computed from the combination of the measured source level per engine face, with the corresponding transfer functions, either measured or computed with SONOR.

$$L_P = 10 * \log 10\left(\sum_f \sum_{source} (P^2 / Q'^2)_{f,source} * Q'^2{}_{f,source} / P_{ref}^2 \right) \quad (26)$$

Figure 12 shows the comparison of measured and computed noise pressure levels for the whole engine, versus the truck position. The trend is respected, and the discrepancies never exceed 2 dBA.

5.4 Intensity maps

In addition to I.L. and pressure spectra, the method enables the plot of intensity maps on the boundary element faces (incident, absorbed, reflected, transmitted and emitted intensities). These outputs can help the shields designer to localize the energy paths and optimize the shields. Figure 13 shows a map of intensity absorbed by the shields of a long distance truck. Figure 14 shows a map of intensity emitted by the engine. A display option in SONOR rending the mesh opaque has been used, in order to illustrate the acoustic leaks, which enable direct acoustic path from the source to the exterior.

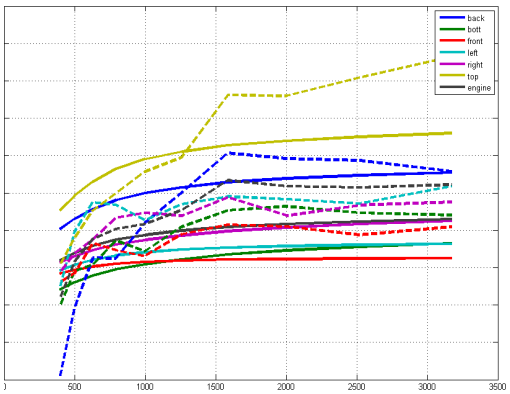

Figure 11 Comparison of Insertion Losses per engine face Solid lines : computed / Dashed lines : measured 2 dB/div.

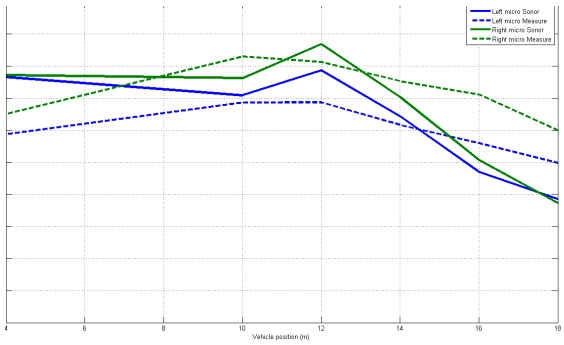

Figure 12 Global pressure levels versus trucks position on the track - constant speed pass-by Solid lines: computed LP / Dashed lines : measured LP 1 dB/division

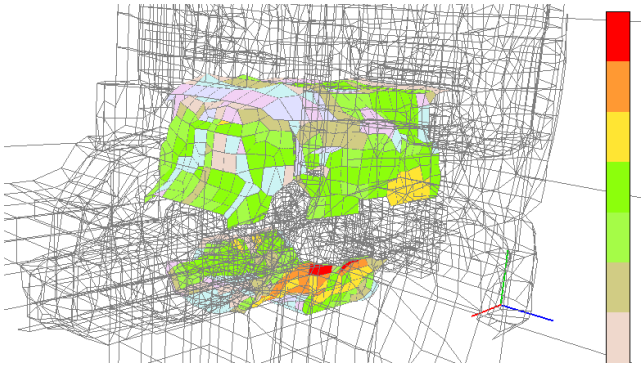

Figure 13 Intensity absorbed by the shields (20 dB dynamic range, 2 dB per colour)

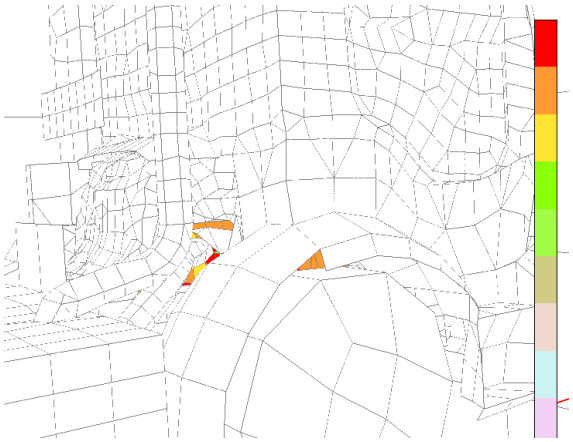

Figure 14 Intensity emitted by the engine (20 dB dynamic range, 2 dB per colour)

6 Interior noise results

This application consists in computing the noise pressure level inside the cabin of a truck, due to the airborne noise generated by the engine.

6.1 Incident intensity

Incident intensity is an interesting intermediate result related to measurable wall pressure levels. A map of computed incident intensity at 1000 Hz is showed on the truck cab panels on Figure 15.

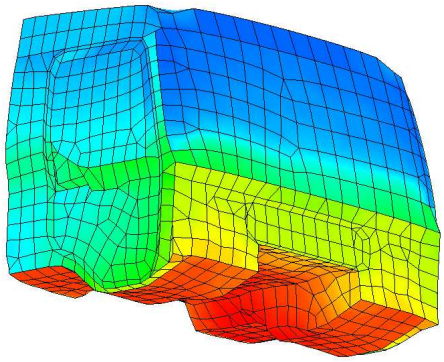

Figure 15 – Incident intensity distribution on the exterior panels of the cab – 1000 Hz – 30 dB dynamic range.

6.2 Interior noise pressure

The next step consists in computing the transmission through the cab panels and the noise radiated inside the cab. Figure 16 shows noise levels at driver ears for 4 different shield configurations. Computed noise spectra (solid lines) are compared with measurement results (dashed lines) issued from the combination of the engine sources with measured airborne noise transfers.

The prediction of noise spectra is correct above 800 Hz and the effect of the shields is well predicted.

Important discrepancies below 800 Hz might be due to misestimated transmission or absorption coefficients, and to modal behaviour in the engine compartment and inside the cab: Sabin critical frequency is around 800 Hz for the cab.

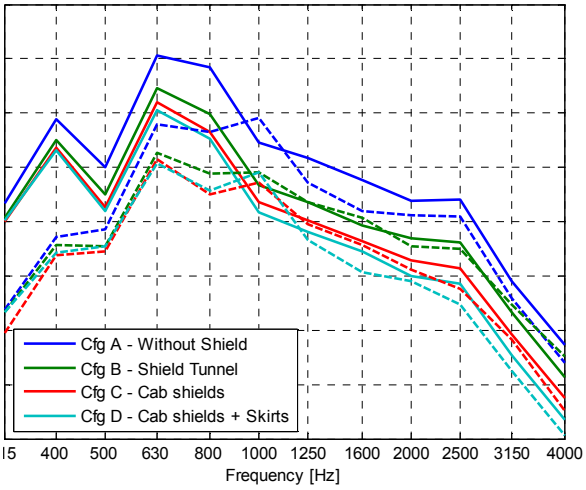

Figure 16: Pressure level inside the cab per shield configuration - Comparison with measurements – dB(A) ref 2e-5 Pa – Full line = using computed transfers – Dash line = using measured transfers – 5 dB/division

7 Conclusion

This paper presents the validation on real trucks, of an acoustic prediction method based on a thermal radiation analogy. A coarse boundary element mesh (5000 elements) is sufficient to describe the geometry. Sources are described by emitted powers and absorbing materials are characterized by classical diffuse absorption and transmission coefficients.

SONOR software, recently developed by VIBRATEC Group, includes pre and post-processing. A cross-validation of this software has been performed by comparison with prior Matlab routines. Acoustic transmission has been implemented and validated.

Multi-cavity optimization and noise pressure computation on point receivers are under development.

The natural output of the computation method is the power absorbed, transmitted and reflected by each element. Insertion Losses (I.L.) are then derived from power balance over element groups. The I.L. can be global (whole engine, whole gearbox) or local (engine faces, components). It characterizes the acoustic efficiency of the shields and can be used to predict power train noise contribution during Pass By Noise tests.

Experimental comparison of both IL and internal noise pressure level show good matching above 800 Hz. Discrepancies below 800 Hz can be explained by modal behaviour, which is neglected in the model. Some differences can also be noticed between the model and the measured truck.

The proposed computation method is reactive and precise and is currently used as a design tool for industrial applications. Computation time is very low.

An adequate boundary element mesh could be used both for classical BEM computation in low frequencies (up to 1000Hz) and for energy BEM computation in high frequencies (800 Hz and above).

Acknowledgements

This work has been carried out with the support of Renault Trucks (a brand of AB Volvo Group).

References

[1] M. Thivant, P. Bouvet, A. Cloix, N. Blairon, Boundary Element Energy Method for the acoustic design of vehicles shields, in Proceeding of ISNVH congress SAE, Graz (2008).

[2] N. Blairon, M. Thivant, Simulation du bruit des véhicules industriels lors de la certification européenne (Pass-by noise), in Proceeding of 3rd congress SIA on Vehicle Comfort, Le Mans (2004).

[3] M. Thivant, Modélisation de la propagation acoustique par la méthode du potentiel d'intensité,. Thèse, Institut National des Sciences Appliquées. 128p. n° d'ordre 03 ISAL 0042, Lyon (2003).

[4] S. Bouvet, Méthode PIANO, livre technique VIBRATEC 900.446.LT13.C (2004).

[5] E. Augis, Mesures sur une maquette d'encapsulage de véhicule industriel suivant une méthodologie de type piano. Rapport VIBRATEC n° 039.090.RA.01.A. (2000).

[6] M. Thivant, A. Cloix, Boundary Element Energy Method for the prediction of machinery encapsulation, Proceedings of SAPEM conference (2005).

[7] A. Le Bot, A vibroacoustic model for high frequency analysis. In Journal of sound and vibration, vol.211, no.4, , p. 537-554 (1998).

[8] A. Le Bot, A. Bocquillet, Comparison of an integral equation on energy and the ray tracing technique for room acoustics. In JASA, vol. 108, no. 4, p. 1732-1740 (2000)

[9] A. Le Bot, E. Reboul, J. Perret-Liaudet, Introduction of acoustical diffraction in the radiative transfer method,. In Comptes rendus mécanique, vol. 332, no. 7, p. 505-511, (2004).

[10] A. Le Bot, E. Reboul, Niveau sonore à 7.5m d'un GMP par le code CERES. In LTDS UMR CNRS 5513, 10 p (2005).

[11] R.F. Lambert, L.Beranek, Sound in large enclosures. In Noise Reduction, p 222-245, USA (1991)